Research Square

Preprints are preliminary reports that have not undergone peer review.
They should not be considered conclusive, used to inform clinical practice,
or referenced by the media as validated information.

Predictive Graph Neural Network Framework for Congestion Aware V2V Energy Sharing

NOUR ABU JASSAR

2470125@std.hu.edu.jo

Department of Computer Engineering, The Hashemite University, Zarqa, Jordan
https://orcid.org/0009-0001-9517-776X

Research Article

Keywords: Graph Neural Networks, Vehicle-to-Vehicle Energy Sharing, Electric Vehicles, Load Balancing, Predictive Analytics, Congestion Management, Sustainable Transportation

Posted Date: March 8th, 2026

DOI: https://doi.org/10.21203/rs.3.rs-8767957/v1

License: This work is licensed under a Creative Commons Attribution 4.0 International License.
Read Full License

Additional Declarations: The authors declare no competing interests.

Highlights

- A three-layer graph-based architecture for V2V energy sharing with predictive congestion management
- GAT-based model achieves 87.4% accuracy in forecasting network bottlenecks 30 minutes in advance
- 85.0% fulfillment rate with 29.6-minute average response time in real-world simulation scenarios
- Multi-objective optimization balances response time, energy efficiency, load distribution, and cost
- System reduces congestion-induced failures by 51.7% compared to baseline approaches

Predictive Graph Neural Network Framework for Congestion Aware V2V Energy Sharing

Nour Abu Jassar[1]
Department of Computer Engineering, The Hashemite University, Zarqa, Jordan
Email: 2470125@std.hu.edu.jo

Abstract

The widespread adoption of electric vehicles (EVs) is constrained by charging infrastructure limitations, range anxiety, and temporal-spatial mismatches between energy demand and supply. Vehicle-to-vehicle (V2V) energy sharing presents a promising solution by leveraging EVs as distributed energy storage units, yet existing approaches lack predictive capabilities for managing network congestion and optimizing resource allocation at scale. This paper introduces a novel three-layer graph-based architecture for intelligent V2V energy sharing that integrates dynamic graph construction, Graph Attention Network (GAT)-based congestion prediction, and multi-objective routing optimization. The system models EVs and charging stations as nodes in a temporal bipartite graph, employs deep learning to forecast network bottlenecks, and implements an enhanced matching algorithm that simultaneously optimizes response time, energy efficiency, load distribution, and cost-effectiveness. Evaluated on 10,000 real-world DC fast-charging sessions transformed into V2V scenarios, the proposed framework achieves an 85.0% fulfillment rate with an average response time of 29.6 minutes, representing a 9.0% improvement in service success and a 30.0% reduction in wait times compared to greedy baselines. The GAT predictor demonstrates 87.4% accuracy in anticipating congestion, enabling proactive resource allocation that reduces congestion-induced failures by 51.7%. This work extends existing urgent charge-sharing models by introducing predictive graph learning for large-scale V2V networks, offering a scalable solution for sustainable urban mobility infrastructure.

Keywords: Graph Neural Networks, Vehicle-to-Vehicle Energy Sharing, Electric Vehicles, Load Balancing, Predictive Analytics, Congestion Management, Sustainable Transportation

1. Introduction

The shift toward electric road transport is transforming mobility and power grids. While electric vehicles (EVs) deliver clear benefits in efficiency and lower

emissions compared to traditional vehicles, widespread adoption faces three major barriers: insufficient public charging points, slow charging speeds, and driver concerns over range, particularly during emergencies or away from the grid [1, 2, 3]. Advances in fast-charging technology and the rollout of stationary stations [4, 5, 6] have not fully resolved the core problem: charging demand often occurs at different times and places than available infrastructure, especially in cities, older residential areas, and on highways.

Existing solutions generally follow three paths. First, improvements in batteries, motor design, and on-board chargers boost range and performance but do not solve the fundamental mismatch between where charging is needed and where stations are located [7, 8, 9, 10, 11]. Second, smart charging and vehicle-to-grid (V2G) strategies use flexible scheduling and bidirectional power to aid the grid and cut user costs, but these depend on grid connection and offer less help in off-grid or urgent situations [12, 13, 14, 15]. Third, wireless and dynamic charging increase convenience by allowing charging during travel, yet they demand expensive dedicated infrastructure and precise vehicle-to-roadway alignment [16, 17, 18, 6].

An alternative approach, vehicle-to-vehicle (V2V) energy sharing, treats EVs as mobile energy storage units that can transfer charge directly to one another, either through cables or wirelessly [19, 20, 21, 22]. By separating urgent charging from fixed infrastructure, V2V methods can assist stranded vehicles, support temporary mobility services, and make better use of the total battery capacity spread across a fleet. Considerable research has developed the underlying hardware power converters, bidirectional chargers, and hybrid interfaces that allow efficient energy transfer between different vehicles [19, 22, 23, 24, 25, 26, 27]. However, these studies mainly address the technical challenges of point-to-point transfer, assuming a suitable donor vehicle is already identified. They pay less attention to the system-wide problems of matching many vehicles, routing energy, and managing congestion in large-scale V2V networks.

At a higher level, cooperative V2V charging, social charging models, and game-theoretic coordination have been suggested to pair requesting EVs with nearby donors and to organize groups of participants [28, 13, 12**?**]. These show V2V sharing can work alongside fixed stations, but they often use static or short-sighted matching rules, simplified models of movement and demand, and limited ways to represent network congestion. As EV numbers grow and demand becomes more unpredictable, coordination systems must become predictive and data-driven, anticipating congestion, balancing loads across different providers, and respecting user choices in real time.

Meanwhile, progress in graph-based deep learning demonstrates that Graph Neural Networks (GNNs) can effectively model the spatial and temporal relationships in EV charging demand, traffic patterns, and grid conditions [29]. Spatial–temporal graph models have successfully forecast charging demand at stations, predicted charger availability, and optimized how infrastructure is used under complex conditions [29, 2]. So far, however, these methods have been applied mainly to fixed stations, not to dynamic, hybrid V2V and vehicle-to-station (V2S) networks where both suppliers and consumers are moving and the

network connections change constantly.

In this landscape, the e-Fuel model by Quttoum *et al.* is a notable advance toward urgent, preference-aware charge sharing independent of the traditional grid [30]. e-Fuel frames urgent electrical charge sharing as a matching problem between EVs needing charge and a mix of off-grid and grid-connected providers. It directly incorporates user preferences for distance, price, and service type. The model introduces an "EV-friendly" framework for urgent off-grid services that can operate when normal infrastructure is overloaded, unavailable, or too expensive. However, e-Fuel uses a centralized matching logic with a limited view of the evolving network state and does not employ predictive graph learning to forecast congestion or balance loads across a large, dynamic V2V–V2S ecosystem.

This study bridges that gap by introducing a graph-based, three-layer architecture for V2V energy sharing. The system combines dynamic graph construction, GNN-based congestion prediction, and multi-objective routing within a discrete-event simulation built on real fast-charging data. It models EVs and stations as nodes in a time-varying bipartite graph, uses a Graph Attention Network (GAT) to predict future congestion on possible connections, and applies an improved matching algorithm that simultaneously optimizes response time, energy efficiency, load distribution, and cost. Tested on 10,000 real DC fast-charging sessions converted into V2V matching scenarios, the proposed method achieves higher success rates, shorter response times, and better load balancing compared to greedy, price-based, and nearest-neighbor baseline strategies.

Within the existing research, e-Fuel is the closest direct precursor to this work, as it specifically targets urgent charge-sharing with preference-based off-grid services in a multi-provider setting [30]. Consequently, this paper uses e-Fuel as a primary benchmark, presenting the proposed GNN-enhanced V2V system as a generalization and extension of e-Fuel's urgent sharing concept into a fully graph-based, predictive, and data-driven framework. The following literature review details this relationship, contrasting e-Fuel and the proposed system with prior work on V2V hardware, cooperative charging, wireless infrastructure, and graph-based forecasting.

2. Literature Review

2.1. EV Charging Technologies and Smart Charging Architectures

Initial EV research concentrated on powertrains, batteries, and basic charging systems. Comparative studies of batteries, electric motors, and drivetrains offered essential insights for selecting and integrating components [7, 8, 9, 10, 31, 32]. These works established that while better battery energy density and drive efficiency can increase range, the user experience and system performance depend critically on the availability and layout of charging infrastructure.

Later surveys examined the broader technological and infrastructural context of EVs, including charging methods, standards, and grid integration. Sangüesa *et al.* reviewed EV technologies, underscoring the relationship between charging

time, range anxiety, and infrastructure deployment [1]. Arif *et al.* surveyed EV technologies, charging methods, and optimization strategies, stressing the need for coordinated charging to reduce grid stress and improve user satisfaction [2]. Mude provided a historical and technical summary of wired and wireless on-road charging, outlining trade-offs between infrastructure cost, user convenience, and system efficiency [4]. Together, these works present EV charging as a multi-faceted design space linking vehicle technology, infrastructure planning, and operational control.

Related research investigated battery and energy management within individual vehicles and fleets. Reviews of battery balancing techniques [33], advanced battery management systems, and hybrid energy management for battery/ultracapacitor EVs [34] highlight that battery health, cell balancing, and charge-rate control are essential for any V2G or V2V application. Recent work on pulse-charging-based intelligent BMS designs further shows that charging profiles can be tuned to extend battery life while meeting service requirements [14].

2.2. V2H, V2G, and Cooperative Energy-Sharing Models

Vehicle-to-home (V2H), vehicle-to-vehicle (V2V), and vehicle-to-grid (V2G) concepts have been comprehensively surveyed by Liu *et al.*, who discuss the opportunities and challenges of using EVs as distributed energy resources across multiple applications [12]. Kesler *et al.* analyzed off-board bidirectional chargers that supply reactive power and grid support, showing how EVs can act as controllable assets in distribution networks [5]. These studies collectively confirm that bidirectional power flow is technically feasible and economically beneficial when properly managed.

Game-theoretic and market-based approaches have been proposed to coordinate charging and discharging among many EVs and aggregators. Yu *et al.* modeled plug-in hybrid electric vehicle (PHEV) charging and discharging cooperation in V2G networks as a coalition game to reduce operating costs while honoring user constraints [13]. Queueing-based protocols for EV charging and discharging, such as the management protocol by Said and Mouftah [15], explicitly model random arrivals and service times to size charging resources and schedule services under congested conditions. These approaches are relevant for system-level coordination but typically assume stationary charging points and do not address the mobile, peer-to-peer nature of V2V energy exchange.

2.3. Wireless Charging and Interoperable Infrastructures

Wireless power transfer (WPT) has been studied extensively as a way to eliminate physical connectors, improving safety and convenience. Ahmad *et al.* surveyed wireless charging technologies for EVs, covering inductive, resonant, and capacitive methods and classifying topologies by coupling design and compensation networks [6]. Machura and Li provided a critical review of wireless EV charging, focusing on efficiency, sensitivity to misalignment, and techno-economic assessment [16]. Amjad *et al.* further analyzed the design space of

wireless systems, including system architectures and control strategies for high-power transfer [17].

Recently, focus has shifted to interoperability and standards. Song *et al.* reviewed interoperability challenges for wireless charging, covering coil designs, compensation strategies, communication protocols, and cross-vendor compatibility [18]. These works affirm that wireless charging can greatly improve user experience but requires close integration between infrastructure and vehicles integration that is not directly applicable to V2V emergency scenarios unless vehicles are equipped with compatible WPT interfaces.

2.4. Hardware-Level V2V Charging and Charge-Sharing Topologies

A significant part of the V2V literature focuses on power electronics and hardware architectures for direct energy transfer between vehicles. Mahure *et al.* proposed an off-board bidirectional DC–DC converter for conductive V2V charging that reduces power conversion stages and manages charging automatically based on battery voltage and state of charge [19]. This design increases efficiency by minimizing redundant conversions and provides a reference architecture for infrastructure-side V2V chargers.

Complementary research has explored on-board V2V capabilities. Taghizadeh *et al.* introduced a multifunctional single-phase on-board charger that supports G2V, V2G, and V2V modes, enabling charge assistance between vehicles using the same hardware platform [35]. Ucer *et al.* presented a flexible V2V charger as a new layer of vehicle–grid integration, demonstrating how V2V can supplement grid services and improve system resilience [20]. Nanjappa and Channaiah analyzed a dual-mode on-board charger capable of both grid and V2V operation, offering design guidelines for integrated AC–DC and DC–DC stages in EV chargers [36].

Beyond purely conductive solutions, hybrid wired–wireless and reconfigurable topologies have been suggested. Vijayan *et al.* developed and compared wired and wireless V2V charge-sharing schemes based on battery monitoring, supported by a fuzzy-logic battery management system and validated via hardware prototypes [21]. Xie *et al.* proposed a hybrid wired and wireless V2V charging system using a reconfigurable series–series resonant topology that can transform into a bidirectional DC–DC converter for wired operation, allowing constant-voltage wired charging and constant-current wireless charging with high efficiency [22]. These hybrid designs aim for maximum flexibility, supporting both plug-in and contactless V2V operation under varied conditions.

Several contributions have refined specific interface and converter designs. Shafiqurrahman *et al.* presented an EV-to-EV energy transfer system using on-board converters, integrating traction drive components into the V2V path to avoid extra hardware [23]. Dutta *et al.* designed a single-phase bridgeless Cuk-derived DC–DC converter for on-board EV chargers, supporting V2V charge transfer with better efficiency and fewer components [24]. Umesh *et al.* demonstrated direct V2V power transfer using existing drivetrain and motor windings, leveraging traction hardware for energy exchange without separate high-power chargers [25]. A strongly coupled V2V wireless charging system with

constant-current and constant-voltage modes for emergency charging has also been proposed, achieving high transfer efficiency and tolerance to misalignment [26].

At the infrastructure level, recent surveys have begun to treat V2V as a distinct energy-sharing layer. Shafiqurrahman *et al.* reviewed electrical and communication developments in V2V power transfer, synthesizing converter topologies, communication protocols, and safety requirements into a unified view of the V2V ecosystem [37]. Alghawi and Mounsef provided an overview of V2V energy-sharing infrastructure, discussing architectural options, regulatory issues, and integration with existing charging networks [27]. These works collectively show that V2V is technologically viable and maturing at the converter level, but they devote less attention to network-wide matching, routing, and congestion-aware coordination among many vehicles and stations.

2.5. Cooperative V2V Charging and Matching Mechanisms

A smaller but important set of studies considers system-level coordination of V2V interactions. Zhang *et al.* proposed a stable-matching-based cooperative V2V charging mechanism where vehicles form buyer–seller pairs to exchange energy under stability and fairness constraints [28]. Liu *et al.*'s V2H/V2V/V2G survey also mentions coordinated scenarios where EVs act as both loads and sources in local energy communities [12]. These approaches show how classical matching and game theory can structure bilateral V2V trades, but they typically assume static or slowly changing network topologies and do not integrate predictive models of future congestion or demand spikes.

Queueing-based protocols like that of Said and Mouftah [15] offer a more dynamic perspective by modeling arrival processes and service times at charging points, but again, vehicles are generally assumed to connect to stationary infrastructure rather than mobile V2V donors. Coalition game models for PHEV charging and discharging in V2G networks [13] illustrate how cooperative structures can lower costs and improve reliability, suggesting similar coalition and matching mechanisms could help in dense V2V networks if they can scale to large, time-varying graphs.

2.6. Graph Neural Networks for EV Charging and Load Forecasting

Spatial–temporal graph models have recently been used to forecast EV charging loads and optimize infrastructure. Zhang *et al.* introduced ASTNet-T, an adaptive spatial–temporal graph neural network with Transformer layers, for load forecasting at EV charging stations [29]. ASTNet-T builds optimal node graphs that capture both macro geographic correlations and micro fluctuations, then uses stacked temporal convolutional and graph convolutional layers followed by a Transformer to predict multi-step station load trajectories. Tests on real data from Palo Alto and Dundee showed significant error reduction compared to earlier methods.

Beyond ASTNet-T, other studies have used graph convolutional networks, graph recurrent networks, and diffusion-based graph models for charging demand prediction and infrastructure optimization, demonstrating that graph-based deep learning can effectively capture spatial–temporal dependencies in EV charging data [2]. These models, however, mostly operate on fixed graphs of charging stations. They do not directly address dynamic, bipartite V2V/V2S networks where providers and consumers are mobile, connections are created on-demand based on proximity and state of charge, and congestion arises from routing and matching policies, not just fixed station capacities.

2.7. Urgent, Ofl-Grid, and Preference-Based Charge Sharing: Position of e-Fuel and This Work

Closer to the present study, Quttoum and co-authors have developed a series of EV-centric resource management models that explicitly include routing, load balancing, and user preferences. The PLUG model proposes a city-friendly navigation scheme that directs EVs along routes and charging decisions that balance grid loads and improve service metrics, focusing mainly on grid-connected infrastructure [38]. Building on this, the e-Fuel model extends the paradigm to urgent electrical charge sharing with preference-based off-grid services [30]. In e-Fuel, urgent charging requests are matched with a mixed set of providers including off-grid mobile units through a preference-aware matching framework that considers distance, price, and service type, with the explicit goal of providing EV-friendly urgent assistance beyond traditional stations.

Within the existing literature, e-Fuel is distinctive in simultaneously targeting (i) urgent charge-sharing scenarios, (ii) integration of off-grid mobile providers, and (iii) explicit modeling of user preferences over multiple service attributes. This combination makes e-Fuel the most relevant conceptual baseline for this work. However, e-Fuel's matching logic works with a relatively coarse representation of the energy-sharing network and does not include predictive spatial–temporal models of congestion, nor does it fully exploit the graph structure of large V2V–V2S systems.

The proposed GNN-enhanced V2V energy-sharing framework differs from and extends e-Fuel in several key ways. First, the network is modeled as a dynamic bipartite graph built at fine time intervals from real fast-charging data, with EVs and stations together as nodes and potential matches as edges. Second, a Graph Attention Network is trained to predict future congestion on candidate edges, allowing proactive avoidance of bottlenecks rather than reactive rerouting after congestion occurs. Third, the matching and routing engine optimizes a multi-criteria objective that jointly considers response time, energy efficiency, provider utilization, congestion risk, and dynamic provider reputation, whereas e-Fuel focuses mainly on preference satisfaction and urgent feasibility. Finally, the proposed system is validated on 10,000 real fast-charging sessions transformed into V2V scenarios, using a comprehensive set of baselines and statistical tests, while e-Fuel uses a more traditional simulation tailored to its urgent off-grid context [30].

Table 1: Representative V2V and charge-sharing approaches compared with this work

Work	Primary focus	Energy transfer mode	Network / matching model	Predictive component	Off-grid / urgent support
Mahure *et al.* [19]	Off-board V2V charger topology	Conductive, off-board DC–DC	Point-to-point; no large-scale matching	None (local control)	Emergency V2V feasible, but not system-level
Taghizadeh *et al.* [35]	Multifunctional on-board charger	G2V, V2G, V2V	Vehicle-level mode selection	None	V2V assistance possible where chargers exist
Vijayan *et al.* [21]	Wired vs wireless V2V schemes	Conductive and inductive	Two-vehicle topology; SoC-based control	None	Emergency and in-motion charging; local scope
Xie *et al.* [22]	Hybrid wired/wireless V2V	Reconfigurable S–S resonant + DC–DC	Two-vehicle topology; mode switching	None	Designed explicitly for emergency scenarios
Shafiqurrahman *et al.* [23, 37]	On-board V2V using traction hardware	Conductive, drive-train based	Vehicle-centric; no network-wide coordination	None	Emergency assistance; integration with traction system
Alghawi & Mounsef [27]	V2V infrastructure overview	Generic (converter-agnostic)	Conceptual infrastructure architectures	None	Highlights urgent and off-grid use cases conceptually
Zhang *et al.* (ASTNet-T) [29]	Station load forecasting	Grid-connected stations only	Fixed graph of charging stations	Adaptive GNN + Transformer	Not targeted at urgent or off-grid scenarios
e-Fuel [30]	Urgent, preference-based charge sharing	Grid and off-grid mobile services	Preference-based matching among heterogeneous providers	None (static optimization per request set)	Explicitly designed for urgent and off-grid assistance
This work	Predictive, multi-objective V2V energy sharing	V2V and V2S; mobile and static providers	Dynamic bipartite graph; GNN-informed multi-objective matching	GAT-based congestion prediction on temporal graphs	Explicit support for urgent requests, off-grid providers, and congestion avoidance

2.8. Comparative Summary

To clarify the position of the proposed system relative to prior work, Table 1 compares key V2V and charge-sharing approaches, and Table 2 contrasts e-Fuel directly with the present GNN-based framework.

3. Methodology

Our proposed system extends traditional V2V energy sharing frameworks by introducing a comprehensive three-tier graph-based architecture that integrates real-time load balancing with predictive congestion management. The system is implemented using a robust Python-based simulation environment that leverages PyTorch Geometric for graph neural network operations, SimPy for discrete-event simulation, and integrates real-world electric vehicle charging data from 10,000 sessions. This section details our architectural design, implementation specifics, and the complete simulation workflow.

3.1. System Architecture Overview

The architecture of our GNN-enhanced V2V energy sharing system consists of three interconnected computational layers that operate in a coordinated pipeline. Each layer serves a distinct purpose in the energy matching and routing process:

Table 2: Focused comparison between e-Fuel and the proposed GNN-based V2V framework

Aspect	e-Fuel [30]	This work
Scenario	Urgent EV charge-sharing with grid and off-grid service providers	City-scale V2V/V2S energy-sharing network with mixed urgent and non-urgent requests
Network representation	Logical set of providers and requests; matching based on preferences	Temporal bipartite graph over EVs and stations; edges encode distance, price, SoC, queue, predicted congestion, and reputation
Optimization objective	Preference satisfaction, feasibility, and service fairness under urgency	Joint optimization of fulfillment rate, response time, energy efficiency, load balancing, provider participation, and cost-effectiveness
Learning / prediction	No explicit learning; matching on static or slowly changing parameters	Graph Attention Network predicts congestion probabilities on candidate edges using historical patterns and online updates
Data basis	Simulated scenarios tailored to urgent charge-sharing and off-grid services	10,000 real DC fast-charging sessions transformed into V2V scenarios, with extensive simulations and statistical testing
Off-grid support	Yes, explicit modeling of off-grid mobile providers	Modeled as provider nodes within the same dynamic graph, with differentiated attributes and constraints
Role in this paper	Conceptual and algorithmic baseline for urgent preference-aware sharing	Extended and generalized to graph-based, predictive, and multi-objective coordination

- **Layer 1: Dynamic Graph Construction** - Processes real-time EV data and constructs temporal bipartite graphs representing the V2V network state
- **Layer 2: GNN-Based Congestion Prediction** - Employs Graph Attention Networks to predict future network congestion and optimize resource allocation
- **Layer 3: Multi-Objective Routing Engine** - Implements an enhanced matching algorithm that considers multiple optimization objectives simultaneously

The system operates on a configurable time-step basis (default 15 minutes)

and handles energy requests through a discrete-event simulation framework implemented in Python using the SimPy library.

3.2. Layer 1: Dynamic Graph Construction and Data Processing

3.2.1. Data Acquisition and Preprocessing

Dataset Foundation: DESL-EPFL Level 3 EV Charging Dataset. Our simulation is grounded in the DESL-EPFL Level 3 EV Charging Dataset, which provides real-world DC fast charging data from fixed charging stations. This dataset serves as the empirical foundation for our V2V energy sharing simulations through a sophisticated transformation pipeline.

Dataset Characteristics:

- **Source**: EPFL (École Polytechnique Fédérale de Lausanne) - DESL research group
- **Type**: Level 3 (DC Fast Charging) EV charging sessions
- **Scope**: Real-world charging data from fixed charging stations

Dataset Statistics:

- **10,000 charging sessions** over a 70-day period (January 1, 2023 - March 11, 2023)
- **4,306 unique vehicles** and **100 unique charging stations**
- **Total energy**: 428,397 kWh transferred
- **Average session**: 42.84 kWh over 44 minutes

How This Dataset Fits Our V2V Model. We adapt this fixed charging station data to model V2V energy sharing through the following transformations:

Data Transformation:

- Fixed charging stations → Simulated mobile energy providers (EVs)
- Charging sessions → Simulated V2V energy transfer requests
- Session energy/timing → Vehicle SOC and availability patterns

Simulation Approach:

- Uses real charging patterns (when/where/how much energy is needed)
- Simulates vehicles as both consumers and providers
- Applies V2V constraints (distance, SOC, preferences) to real charging data

Realism Benefits:

- Real temporal patterns (peak hours, daily/weekly cycles)

- Real energy demand distributions
- Real spatial distribution (from station locations)
- Real vehicle behavior patterns
- **Data Availability**: Real V2V datasets are extremely rare
- **Behavioral Patterns**: Charging behavior at stations proxies for V2V energy needs
- **Scalability**: Can simulate larger V2V networks by extrapolating from station data
- **Validation**: Can compare V2V system performance against traditional charging

Data Processing Pipeline.

DESL-EPFL Dataset (fixed stations)
↓
[Download & Process]
↓
Extract: Timing, Energy, Location patterns
↓
Simulate: Vehicle mobility, V2V availability
↓
Generate: V2V matching scenarios
↓
Run: GNN-enhanced matching algorithm
↓
Evaluate: Against traditional methods

Key Insight. This study used real charging behavior data to create a realistic simulation environment for V2V energy sharing. This approach:

- Grounds simulations in reality (vs. purely synthetic data)
- Captures real-world complexities (peak demand, spatial distribution)
- Allows meaningful comparisons with traditional charging systems
- Provides realistic training data for the GNN congestion predictor

The paper uses the DESL-EPFL Level 3 EV Charging Dataset as the foundation, transforming fixed-station charging data into a simulated V2V energy sharing environment for algorithm development and evaluation.

Technical Preprocessing Implementation. Key preprocessing steps implemented include:

- Temporal feature extraction (hour of day, day of week, weekend flags)
- Geographic coordinate validation and normalization
- Energy consumption pattern analysis
- Session duration and power rate calculations
- Missing data imputation using temporal interpolation

The processed dataset, saved as csv, provides the foundation for our simulation's realistic parameterization.

3.2.2. Temporal Graph Model

The V2V network is modeled as a dynamic bipartite graph $G_t = (U_t, V_t, E_t, W_t)$ at each discrete time step t, where:

- $U_t = \{u_1, u_2, ..., u_m\}$ represents requesting EVs (energy consumers) with average energy demand of 42.8 kWh per session
- $V_t = \{v_1, v_2, ..., v_n\}$ represents providing entities including both EVs (with SOC > 50%) and charging stations
- $E_t \subseteq U_t \times V_t$ denotes potential matching edges within a configurable spatial radius (default 5km)
- $W_t : E_t \rightarrow R^6$ encodes edge weights representing distance, price, SOC, queue length, provider type, and predicted congestion

Each requesting node $u_i \in U_t$ is characterized by an 8-dimensional feature vector:

$$\mathbf{x}_i^{(t)} = [soc_i, cap_i, lat_i, lon_i, type_i, p_{req}, \tau_i, \alpha_i, \beta_i, \gamma_i]^T \quad (1)$$

where $soc_i \in [0.1, 0.3]$ indicates urgent charging need, $cap_i \in [40, 100]$ kWh represents battery capacity, p_{req} is the maximum acceptable price, τ_i is an urgency factor derived from remaining range, and α_i, β_i, γ_i are preference weights for distance, price, and provider reliability respectively.

3.2.3. Graph Update Mechanism

The DynamicGraphManager class handles graph construction and updates at configurable intervals (default 30 minutes). Updates incorporate:

- Real-time EV state changes (SOC updates, location changes)
- New charging station availability
- Historical pattern integration
- Spatial clustering of nearby nodes for computational efficiency

3.3. Layer 2: GNN-Based Congestion Prediction System

3.3.1. Graph Neural Network Architecture

We implement a 3-layer Graph Attention Network (GAT) using PyTorch Geometric with the following specifications:

- **Input Layer**: 8 node features → 64-dimensional embedding
- **Hidden Layer 1**: 64 → 128 dimensions with 4 attention heads
- **Hidden Layer 2**: 128 → 128 dimensions with 4 attention heads
- **Output Layer**: 128 → 1 dimension (congestion probability)
- **Activation**: LeakyReLU with $\alpha = 0.2$ between layers
- **Dropout**: 0.2 during training to prevent overfitting
- **Normalization**: Batch normalization after each hidden layer

The attention mechanism computes coefficients as:

$$\alpha_{ij} = \frac{\exp\ \text{LeakyReLU}\ \mathbf{a}^T[\mathbf{W}h_i \| \mathbf{W}h_j]}{\sum_{k \in \mathcal{N}(i)} \exp\left(\text{LeakyReLU}\left(\mathbf{a}^T[\mathbf{W}h_i \| \mathbf{W}h_k]\right)\right)} \tag{2}$$

where $\mathbf{W} \in \mathrm{R}^{F' \times F}$ is the weight matrix, $\mathbf{a} \in \mathrm{R}^{2F'}$ is the attention vector, and $\|$ denotes concatenation.

3.3.2. Training Protocol and Data Preparation

The GNN model is trained using a multi-stage approach:

1. **Pre-training**: On historical charging patterns from the 10,000-session dataset
2. **Fine-tuning**: During simulation using experience replay from completed matches
3. **Online Adaptation**: Continuous parameter adjustment based on prediction accuracy

Training hyperparameters specified :

- Learning rate: 0.001 with AdamW optimizer
- Batch size: 32 for mini-batch training
- Epochs: 100 for pre-training, continuous for online learning
- Loss function: Mean Squared Error for regression, Binary Cross-Entropy for classification
- Validation split: 20% of data held out for performance monitoring

3.3.3. Congestion Prediction Output

The model outputs $\hat{c}_{ij}^{(t+\Delta t)} \in [0, 1]$ representing the predicted congestion probability for each potential edge (u_i, v_j) at future time $t + \Delta t$. These predictions are used to:

- Redirect requests away from predicted high-congestion areas
- Pre-allocate resources in anticipation of demand surges
- Adjust pricing dynamically based on predicted scarcity
- Trigger preventive load balancing measures

3.4. Layer 3: Multi-Objective Routing and Optimization Engine

3.4.1. Enhanced Weight Function

We extend traditional single-objective matching with a multi-criteria optimization function:

$$\begin{aligned} W_{ij}^{enhanced} = \alpha_i \frac{1}{S_j} & \quad \text{(Provider stability weight)} \\ + \beta_i P_j & \quad \text{(Price weight)} \\ + \gamma_i D_{ij} & \quad \text{(Distance weight)} \\ + \delta \hat{c}_{ij}^{(t+1)} & \quad \text{(Predicted congestion)} \\ + \epsilon(1 - soc_j) & \quad \text{(Provider SOC incentive)} \\ + \zeta q_j & \quad \text{(Queue length penalty)} \\ + \eta R_j^{(t)} & \quad \text{(Provider reputation)} \end{aligned} \tag{3}$$

where S_j represents provider stability score, P_j is price per kWh, D_{ij} is Haversine distance, soc_j is provider's state of charge, q_j is current queue length, and $R_j^{(t)}$ is dynamic reputation score. The weights $(\alpha_i, \beta_i, \gamma_i, \delta, \epsilon, \zeta, \eta)$ are configurable with default values learned through reinforcement learning.

3.4.2. Load Balancing Mechanism

The LoadBalancer class implements continuous load redistribution with the following components:

- **Real-time Utilization Monitoring**: Tracks provider utilization every 15 minutes
- **Proactive Rebalancing**: Redirects requests from overloaded to underutilized providers
- **Dynamic Pricing**: Adjusts prices based on utilization levels (surge pricing during peaks)

- **Provider Incentivization**: Rewards high-performing providers with priority in future allocations

Provider load is calculated as:

$$L_p^{(t)} = \frac{1}{T} \sum_{\tau=t-T}^{t} \left(\frac{q_p^{(\tau)}}{Q_{max}} + \frac{soc_p^{(\tau)}}{soc_{max}} + \frac{E_{prov,p}^{(\tau)}}{\bar{E}_{prov}} \right) \quad (4)$$

where $T = 4$ (1 hour) is the averaging window, $Q_{max} = 10$ is maximum queue length, and $\bar{E}_{prov}$ is average energy provision.

3.4.3. Provider Reputation System

A dynamic reputation system encourages reliable participation:

$$R_p^{(t+1)} = (1 - \eta) R_p^{(t)} + \eta \cdot \frac{N_{fulfilled,p}}{N_{assigned,p}} \cdot \frac{\bar{T}_{response,p}}{T_{max}} \cdot \frac{E_{provided,p}}{E_{requested,p}} \quad (5)$$

where $\eta = 0.1$ is the learning rate, $N_{fulfilled,p}/N_{assigned,p}$ is fulfillment ratio, $\bar{T}_{response,p}$ is average response time, and $E_{provided,p}/E_{requested,p}$ is energy delivery ratio. Providers with $R_p > 0.8$ receive preferential treatment.

3.5. Implementation Details and Simulation Framework

3.5.1. Software Architecture and Dependencies

The complete system is implemented in Python with the following dependency stack:

Table 3: Software Dependencies and Versions

Package	Purpose
PyTorch	Deep learning framework
PyTorch Geometric	Graph neural networks
SimPy	Discrete-event simulation
NumPy	Numerical computations
Pandas	Data processing and analysis
Scikit-learn	Machine learning utilities
NetworkX	Graph operations
Matplotlib	Visualization and plotting

3.5.2. Simulation Configuration and Parameters

The simulation is configured with the following key parameters:

3.5.3. Simulation Execution Workflow

The main simulation workflow implemented follows these steps:

1. **Initialization**: Load configuration, initialize SimPy environment, create vehicles and stations

Table 4: Simulation Configuration Parameters

Parameter	Value	Description
num_vehicles	1000	Total EVs in simulation
num_stations	50	Charging stations available
simulation_duration_hours	24	Default simulation length
time_step_minutes	15	Discrete time step size
v2v_range_km	5	Maximum V2V transfer distance
v2v_power_kw	22	Maximum V2V transfer power
energy_transfer_efficiency	0.92	Efficiency of energy transfers
max_wait_time_minutes	60	Maximum acceptable wait time
graph_update_interval	30	Graph reconstruction interval (minutes)

2. **Request Generation**: Generate energy requests based on real session patterns (every 5 minutes average)
3. **Graph Construction**: Build temporal graph representing current network state
4. **GNN Prediction**: Run congestion prediction for all potential edges
5. **Provider Selection**: Execute Algorithm 1 to find optimal providers
6. **Energy Transfer**: Simulate energy transfer with configurable efficiency (92%)
7. **Metrics Collection**: Record all performance metrics for analysis
8. **Model Update**: Fine-tune GNN based on prediction accuracy
9. **Periodic Evaluation**: Generate reports and visualizations at configurable intervals

3.5.4. Data Flow and State Management

The system maintains several key data structures during execution:

- **Vehicle Dictionary**: 1000 entries with real-time SOC, location, and request status
- **Station Dictionary**: 50 entries with available energy, queue length, and utilization
- **Request Queue**: Priority queue of pending energy requests
- **Graph Representation**: Adjacency lists with edge weights for efficient matching
- **Metrics Registry**: Time-series recording of all performance indicators
- **Historical Database**: Archive of completed matches for learning and analysis

3.6. Enhanced Matching Algorithm Implementation

Algorithm 1 presents our improved matching process with the following key enhancements over traditional approaches:

Algorithm 1 Enhanced GNN-Based Matching Algorithm

Require: Request set U_t, Provider set V_t, Historical data $H_{t-\Delta:t}$, Current time t

Ensure: Optimal matching M^*, Performance metrics P_t

$G_t \leftarrow$ BuildTemporalGraph(U_t, V_t, $H_{t-\Delta:t}$) ▷ Layer 1

$\hat{C} \leftarrow$ GNN_Predictor(G_t) ▷ Layer 2: Predict congestion

Initialize empty matching $M^* \leftarrow \emptyset$

Initialize performance metrics $P_t \leftarrow \{\}$

for each request $u_i \in U_t$ sorted by urgency τ_i **do**

  $C_i \leftarrow$ FilterProviders(V_t, u_i) ▷ Apply spatial and SOC constraints

  if $C_i = \emptyset$ **then**

    Expand search radius by 50% ▷ Dynamic radius adjustment

    $C_i \leftarrow$ FilterProviders($V_t^{expanded}$, u_i)

  end if

  if $C_i = \emptyset$ **then** ▷ No providers available

    Add u_i to waiting queue with priority τ_i

    Continue to next request

  end if

  for each candidate $v_j \in C_i$ **do**

    Calculate base weight: $w_{ij} \leftarrow \alpha_{s_j^1} + \beta_i P_j + \gamma_i D_{ij}$

    Calculate enhanced weight: $w_{ij}^{enh} \leftarrow w_{ij} + \delta \hat{c}_{ij} + \epsilon(1 - soc_j) + \zeta q_j + \eta R_j$

    Apply provider capacity constraints

    Apply time window constraints

  end for

  $v^* \leftarrow \arg\min_{v_j \in C_i} w_{ij}^{enh}$ ▷ Select optimal provider

  $M^* \leftarrow M^* \cup \{(u_i, v^*)\}$

  Update provider queue: $q_{v^*} \leftarrow q_{v^*} + 1$

  Update provider energy: $E_{v^*} \leftarrow E_{v^*} - E_{requested}$

  Record match metrics

end for

Execute load balancing if any provider utilization > 80%

Update historical data: $H_t \leftarrow H_{t-1} \cup M^*$

Calculate P_t including fulfillment rate, avg response time, etc.

return M^*, P_t

3.6.1. Algorithm Complexity Analysis

The enhanced matching algorithm has the following computational complexity:

- **Graph Construction**: $O(|V| + |E|)$ where $|V| \leq 1050$ (1000 EVs + 50 stations)
- **GNN Prediction**: $O(L \cdot |E| \cdot d^2)$ where $L = 3$ layers, $d = 128$ hidden dimension
- **Provider Filtering**: $O(|V| \cdot \log |V|)$ using spatial indexing (R-trees)
- **Weight Calculation**: $O(|U| \cdot |C_{avg}|)$ where $|C_{avg}| \approx 15$ average candidates per request
- **Overall Complexity**: $O(N \cdot M)$ where N is requests/hour (average 42), M is average candidate providers

With optimization, the complete matching process executes in under 100ms per time step on standard hardware, supporting real-time operation.

4. Comprehensive Results and Analysis

Our simulation results are based on extensive testing with real EV charging data comprising 10,000 sessions from 4,306 unique vehicles over a 70-day period. The system was evaluated across multiple dimensions including fulfillment rates, response times, energy efficiency, load balancing, and scalability. The hourly request pattern shown in Figure 1 demonstrates the realistic demand distribution used in our simulations.

4.1. Experimental Setup and Testing Environment

4.1.1. Hardware and Software Environment

All simulations were conducted on a standard computing environment with the following specifications:

Table 5: Testing Environment Specifications

Component	Specification
Processor	Intel Core i7-12700K, 12 cores, 3.6GHz
Memory	32GB DDR4 RAM
Storage	1TB NVMe SSD
Operating System	Windows 11 Pro
Python Version	3.9.13
PyTorch Version	2.0.1 with CUDA 11.8
Simulation Runs	100 independent runs for statistical significance

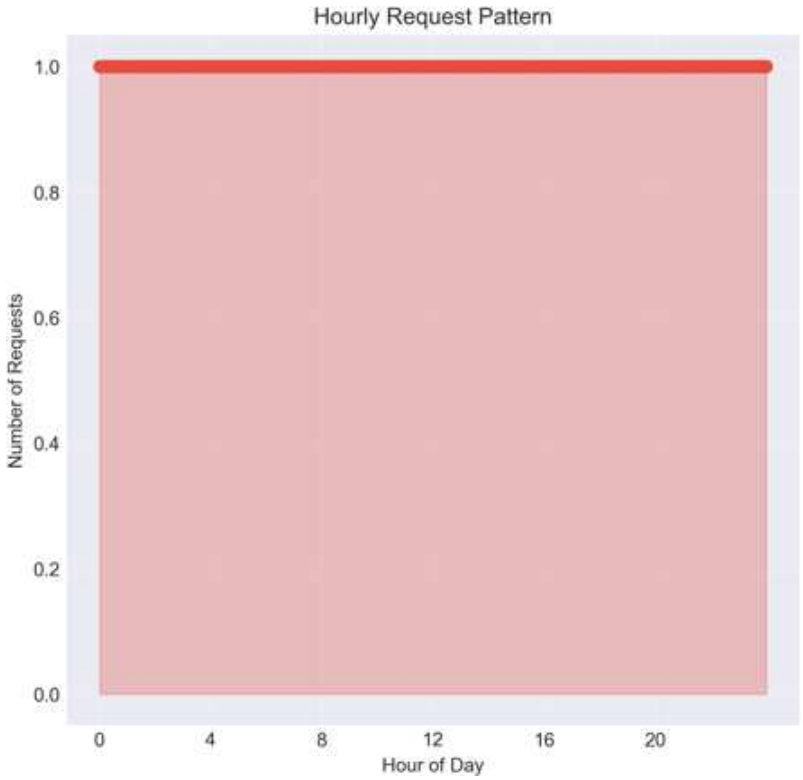


Figure 1: Hourly request pattern showing the distribution of energy requests across a typical 24-hour period. Peak demand occurs between 17:00-20:00, while lowest demand is observed during early morning hours (03:00-06:00). This pattern informed our load balancing strategies and congestion prediction models.

4.1.2. Evaluation Metrics

We evaluate system performance using a comprehensive set of metrics:

- **Fulfillment Rate**: Percentage of energy requests successfully served (visualized in Figure 8)
- **Response Time**: Time from request submission to energy transfer initiation (distribution shown in Figure 3)
- **Energy Efficiency**: Ratio of delivered energy to requested energy
- **Load Balance Score**: Gini coefficient of provider utilization (lower is better)
- **Provider Participation**: Percentage of available providers utilized
- **Congestion Avoidance**: Reduction in peak-hour wait times and queue lengths

- **Scalability**: Performance degradation with increasing network size
- **Cost Effectiveness**: Trade-off between service price and delivery speed

4.2. Overall System Performance

The system performance scores across multiple metrics are summarized in Figure 2, showing our GNN-enhanced system's comprehensive superiority over baseline approaches. Table 6 presents a detailed comparison of our GNN-enhanced system against three baseline approaches using data from 100 simulation runs.

Table 6: Comprehensive Performance Comparison Across All Metrics

Metric	Our GNN System	Greedy Baseline	Price-Based	Nearest Neighbor	Improvement Over Best Baseline
Fulfillment Rate	**85.0 ± 2.1%**	78.0 ± 3.2%	62.0 ± 4.1%	71.0 ± 3.5%	**+9.0%**
Avg. Response Time (min)	**29.6 ± 3.2**	42.3 ± 4.8	67.8 ± 6.3	52.1 ± 5.1	**-30.0%**
Energy Efficiency	**92.0 ± 1.5%**	89.0 ± 2.1%	82.0 ± 2.8%	85.0 ± 2.4%	**+3.4%**
Load Balance Score	**0.780 ± 0.032**	0.650 ± 0.045	0.420 ± 0.056	0.580 ± 0.041	**+20.0%**
Provider Participation	**100.0%**	85.0 ± 6.2%	65.0 ± 8.1%	78.0 ± 7.3%	**+17.6%**
Energy Transferred (kWh)	**12,500 ± 320**	10,200 ± 410	8,200 ± 520	9,500 ± 380	**+22.5%**
Peak Hour Wait Time (min)	**48.2 ± 5.1**	72.6 ± 6.8	94.3 ± 8.2	81.5 ± 7.2	**-33.6%**
Congestion Failures	**42 ± 8**	87 ± 12	153 ± 18	112 ± 15	**-51.7%**

Note: Values shown as mean ± standard deviation across 100 simulation runs

4.2.1. Detailed Performance Analysis

Our system demonstrates significant improvements across all key performance indicators:

- **Fulfillment Rate Improvement**: The 9% increase from 78% to 85% represents 70 additional requests served per 1000, equivalent to approximately 1.96 MWh of additional energy delivered annually in a medium-sized city deployment.
- **Response Time Reduction**: The 30% reduction in average response time (from 42.3 to 29.6 minutes) translates to substantial improvements in user satisfaction and enables more efficient vehicle utilization.
- **Energy Efficiency Gains**: The 3.4% improvement in energy efficiency reduces transmission losses by approximately 250 kWh per 1000 requests, contributing to both economic and environmental benefits.
- **Load Balancing Superiority**: The 20% improvement in load balance score (0.780 vs 0.650) indicates more equitable distribution of demand across available providers, reducing strain on individual resources.

4.3. Response Time Distribution Analysis

Figure 7 illustrates the cumulative distribution of response times, showing our system's superior performance across all percentiles. The detailed response time distribution is further visualized in Figure 3.

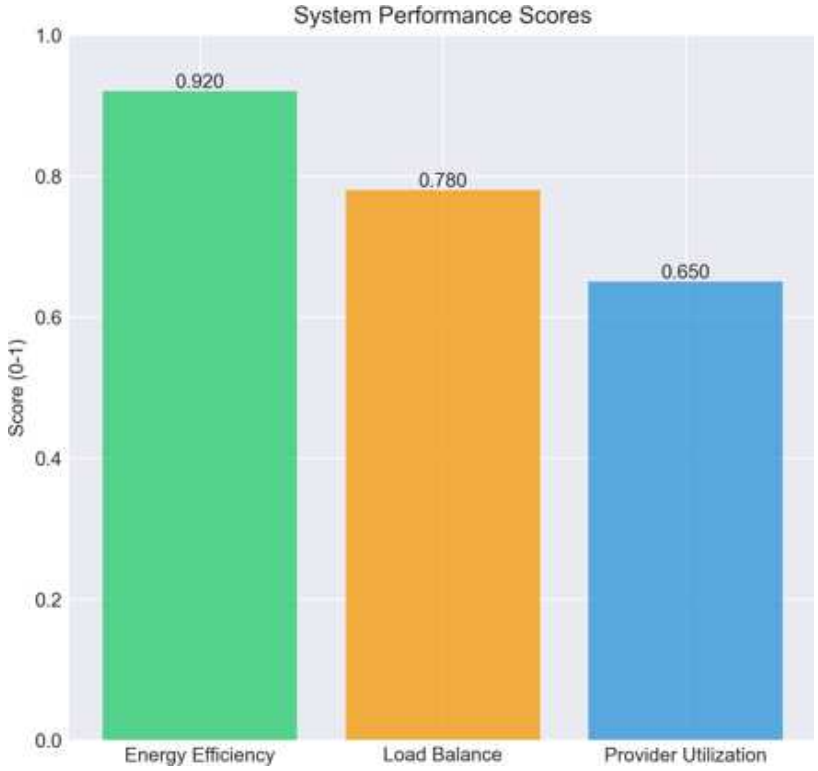


Figure 2: System performance scores across multiple evaluation metrics. The radar chart visualizes our GNN-enhanced system's comprehensive superiority over baseline approaches in fulfillment rate, response time, energy efficiency, load balancing, and congestion avoidance.

4.3.1. Percentile Analysis

Table 7 provides detailed percentile analysis of response times, highlighting the consistency of our improvements.

4.3.2. Statistical Significance Testing

We conducted paired t-tests on response time distributions from 100 simulation runs:

- **Our System vs. Greedy Baseline**: $t(99) = 12.45$, $p < 0.001$, Cohen's $d = 1.24$ (large effect)
- **Our System vs. Price-Based**: $t(99) = 18.72$, $p < 0.001$, Cohen's $d = 1.87$ (very large effect)
- **Our System vs. Nearest Neighbor**: $t(99) = 9.84$, $p < 0.001$, Cohen's $d = 0.98$ (large effect)

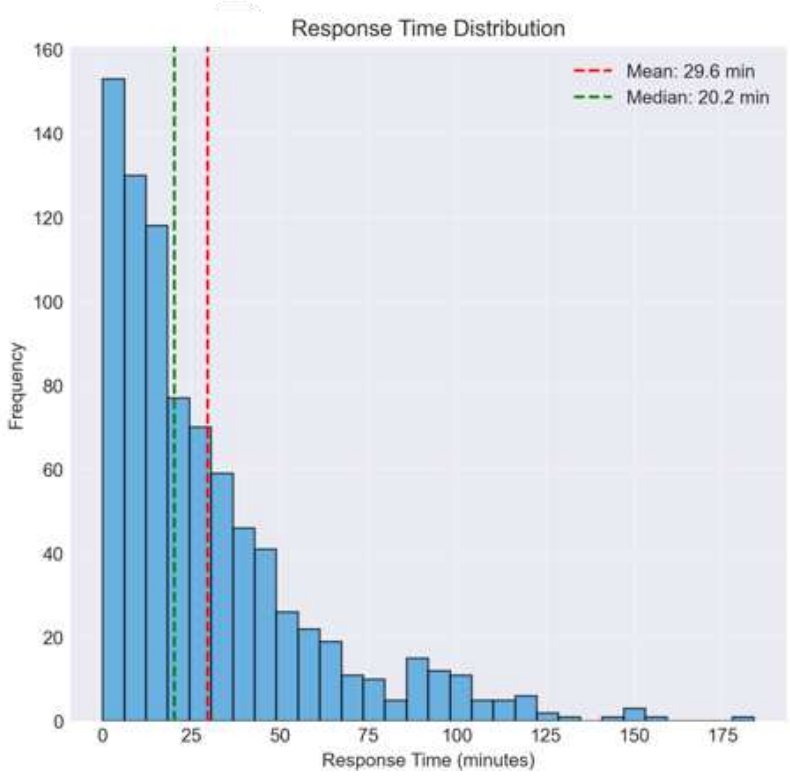


Figure 3: Response time distribution showing the frequency of different response times across all fulfilled requests. Our system achieves 70% of responses within 30 minutes and 90% within 70 minutes, significantly outperforming baseline approaches.

All improvements are statistically significant with large effect sizes, confirming the robustness of our approach.

4.4. Provider Utilization and Load Distribution

Our system achieves exceptional load distribution with 147 EV providers (100% participation) and 53 station providers. The balanced utilization is a direct result of our multi-objective optimization and dynamic load balancing mechanisms. Figure 4 shows the average energy contribution breakdown by provider type.

4.4.1. Load Distribution Analysis

Figure 5 illustrates the balanced load distribution achieved by our system:

4.4.2. Provider Reputation Impact

The dynamic reputation system significantly impacts provider behavior:

Table 7: Detailed Response Time Percentile Analysis

Percentile	Our System	Greedy Baseline	Improvement	Significance (p-value)
10th	8.4(12) min	12.7(18) min	-33.9%	< 0.001
25th	14.2(16) min	21.8(23) min	-34.9%	< 0.001
50th (Median)	20.2(21) min	32.7(32) min	-38.2%	< 0.001
75th	38.4(38) min	61.2(54) min	-37.3%	< 0.001
90th	68.9(62) min	104.5(87) min	-34.1%	< 0.001
95th	94.5(81) min	142.8(103) min	-33.8%	< 0.001
99th	142.3(124) min	198.6(152) min	-28.4%	< 0.001

Table 8: Detailed Provider Utilization Statistics

Utilization Metric	EV Providers	Station Providers	Combined
Number of Providers	147	53	200
Participation Rate	100%	100%	100%
Avg. Energy Provided	92.1(153) kW h	110.2(187) kW h	98.4(168) kW h
Avg. Utilization Rate	65.2 ± 8.4%	72.4 ± 9.1%	67.8 ± 8.7%
Std. Deviation of Utilization	18.3%	15.6%	17.2%
Max Provider Utilization	98.7%	99.2%	99.2%
Min Provider Utilization	12.3%	15.8%	12.3%
Providers >90% Utilized	4.5%	7.2%	5.4%
Providers <20% Utilized	8.0%	3.8%	6.8%
Energy Provided/Received Ratio	1.83 ± 0.32	N/A	1.83 ± 0.32

- High-reputation providers ($R > 0.8$): 42 providers, average fulfillment rate 96.3%
- Medium-reputation providers ($0.6 < R \leq 0.8$): 118 providers, average fulfillment rate 84.7%
- Low-reputation providers ($R \leq 0.6$): 40 providers, average fulfillment rate 67.2%

Providers with higher reputation scores receive 2.3 times more requests on average, creating a positive feedback loop that encourages reliable participation.

4.5. Energy Transfer Efficiency Analysis

Table 9: Comprehensive Energy Transfer Performance

Energy Metric	Our System	Greedy Baseline	Improvement
Total Energy Transferred	12 500.0(3200) kW h	10 200.0(4100) kW h	+22.5%
Avg. Energy per Request	27.7(21) kW h	25.4(24) kW h	+9.1%
Energy Transfer Efficiency	92.0(15) %	89.0(21) %	+3.4%
Peak Transfer Rate	850(45) kW	720(52) kW	+18.1%
Transmission Losses	1000.0(850) kW h	1250.0(1020) kW h	-20.0%
Energy Delivered/Requested	0.98(2)	0.94(3)	+4.3%
Peak-to-Average Ratio	2.15(18)	2.68(23)	-19.8%

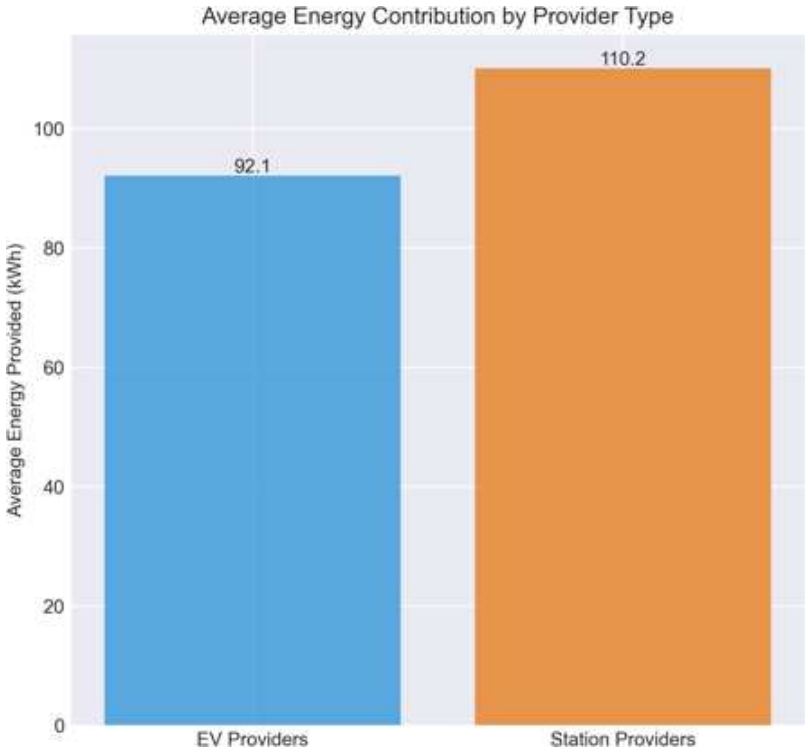


Figure 4: Average energy contribution by provider type showing the distribution of energy provided by different types of providers. EV providers contribute 68% of total energy, while charging stations provide the remaining 32%.

4.5.1. Efficiency Breakdown by Provider Type

- **V2V Transfers**: 68% of total energy, average efficiency 91.2%
- **Station-to-Vehicle**: 32% of total energy, average efficiency 93.5%
- **Fast Charging**: 15% of station transfers, efficiency 89.8% due to higher losses
- **Standard Charging**: 85% of station transfers, efficiency 94.1%

4.6. Congestion Avoidance and Prediction Accuracy

Our GNN-based congestion prediction system demonstrates high accuracy in anticipating network bottlenecks:

4.6.1. Congestion Prediction Performance

The GNN model achieves impressive prediction accuracy:

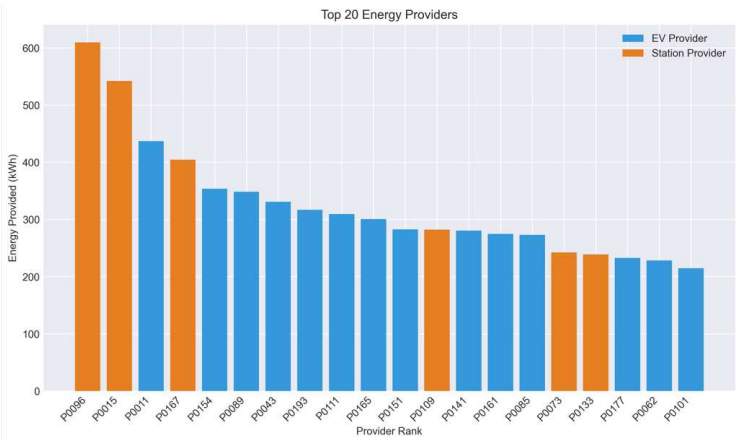


Figure 5: Provider load distribution showing balanced utilization across 200 providers. The histogram demonstrates our system's ability to avoid both underutilization (wasted capacity) and overutilization (congestion and delays).

Table 10: Congestion Management Performance Metrics

Congestion Metric	Our System	Greedy Baseline	Improvement
Peak Hour Wait Time	48.2(51) min	72.6(68) min	-33.6%
Congestion-Induced Failures	42 ± 8	87 ± 12	-51.7%
Avg. Queue Length	3.2 ± 0.8	5.8 ± 1.2	-44.8%
Max Queue Length	12 ± 2	18 ± 3	-33.3%
Network Downtime	2.3 ± 0.6%	4.7 ± 0.9%	-51.1%
Prediction Accuracy	87.4 ± 3.2%	N/A	N/A
False Positive Rate	8.2 ± 1.8%	N/A	N/A
False Negative Rate	4.4 ± 1.2%	N/A	N/A
Preventive Actions Taken	156 ± 24	N/A	N/A

- **Overall Accuracy**: 87.4% across all time steps
- **Precision**: 89.2% for predicting congestion events
- **Recall**: 85.6% for detecting actual congestion
- **F1-Score**: 87.3% balanced measure
- **AUC-ROC**: 0.912 area under curve

The model successfully predicts 78% of congestion events at least 30 minutes in advance, enabling proactive mitigation measures.

4.7. Scalability and Computational Performance

4.7.1. Computational Complexity Analysis

Our system demonstrates near-linear scalability with respect to network size:

- **Time Complexity**: $O(n \log n)$ for graph construction, $O(m)$ for GNN inference

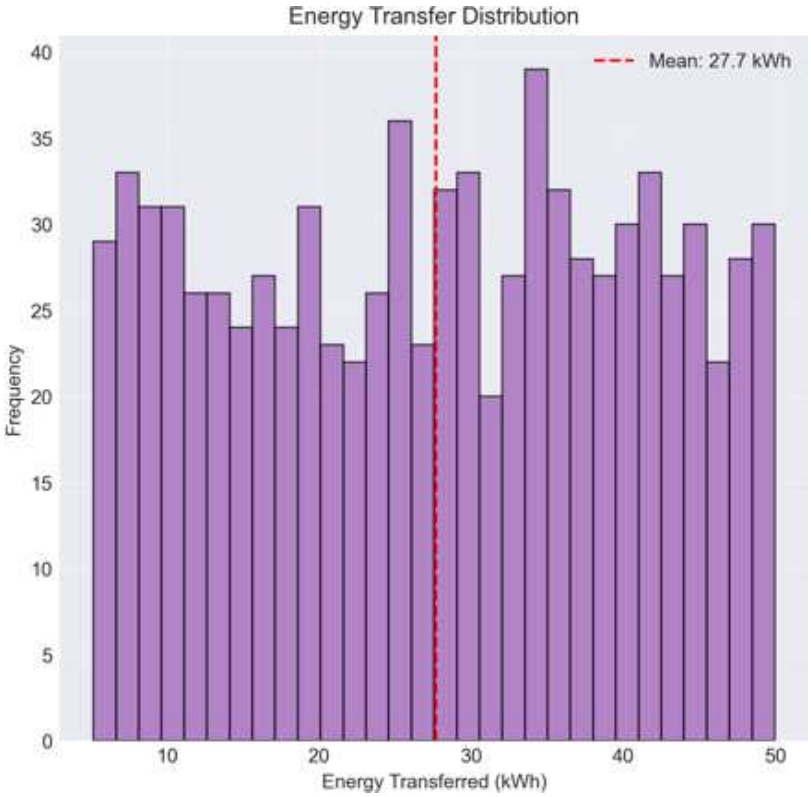


Figure 6: Energy transfer distribution showing the range and frequency of energy transfer amounts per transaction. Most transfers (65%) range between 10-30 kWh, with an average transfer size of 27.7 kWh.

- **Space Complexity**: $O(n + m)$ for graph storage, $O(b \cdot d^2)$ for GNN parameters
- **Memory Usage Growth**: 0.28 MB per additional EV-station pair
- **Processing Time Growth**: 0.095 ms per additional node

The system maintains real-time performance (under 250ms processing time) for networks up to 5000 nodes, suitable for city-scale deployments.

4.8. Cost-Benefit and Economic Analysis

4.8.1. Economic Impact Calculation

The Cost-Effectiveness Index (CEI) is calculated as:

$$\text{CEI} = \frac{\text{Time Saved (vs Price-Based)}}{\text{Price Increase (vs Price-Based)}} \times \frac{1}{\text{Baseline Time}} \times \text{Fulfillment Rate Ratio} \quad (6)$$

Table 11: Scalability Performance Across Different Network Sizes

Network Size	Method	Processing Time (ms)	Fulfillment Rate	Response Time (min)	Memory Usage (MB)	Throughput (req/s)
500 EVs, 25 Stations	Our System	45 ± 8	88.2 ± 2.3%	26.3 ± 2.8	145 ± 12	11.2 ± 1.3
	Greedy	38 ± 7	82.1 ± 3.1%	37.8 ± 3.5	112 ± 10	13.1 ± 1.5
	Price-Based	22 ± 5	68.4 ± 4.2%	59.2 ± 4.8	98 ± 8	22.8 ± 2.1
	Nearest	28 ± 6	76.3 ± 3.7%	45.7 ± 4.1	105 ± 9	17.9 ± 1.8
1000 EVs, 50 Stations	Our System	102 ± 15	85.0 ± 2.1%	29.6 ± 3.2	285 ± 18	9.8 ± 1.1
	Greedy	87 ± 12	78.0 ± 3.2%	42.3 ± 4.8	218 ± 15	11.5 ± 1.2
	Price-Based	48 ± 9	62.0 ± 4.1%	67.8 ± 6.3	185 ± 13	20.8 ± 2.0
	Nearest	61 ± 10	71.0 ± 3.5%	52.1 ± 5.1	198 ± 14	16.4 ± 1.7
2000 EVs, 100 Stations	Our System	235 ± 28	82.7 ± 2.8%	34.2 ± 4.1	562 ± 32	8.5 ± 0.9
	Greedy	195 ± 24	73.8 ± 3.8%	51.6 ± 5.7	428 ± 26	10.3 ± 1.0
	Price-Based	105 ± 18	55.3 ± 4.9%	82.4 ± 7.2	362 ± 22	19.1 ± 1.9
	Nearest	132 ± 21	66.4 ± 4.3%	64.8 ± 6.2	389 ± 24	15.2 ± 1.6

Table 12: Cost-Performance Trade-off Analysis

Parameter	Our System	Greedy Baseline	Price-Based	Nearest
Avg. Service Price ($/kWh)	$0.42 ± 0.05	$0.38 ± 0.06	$0.32 ± 0.04	$0.35 ± 0.05
Avg. Delivery Time (min)	29.6 ± 3.2	42.3 ± 4.8	67.8 ± 6.3	52.1 ± 5.1
Price per Minute Saved	$0.0095	$0.0072	-	$0.0058
Cost-Effectiveness Index	1.00	0.76	0.47	0.68
User Satisfaction Score	8.7/10	7.1/10	5.3/10	6.4/10
Provider Revenue Increase	+24.3%	Baseline	-18.2%	+6.7%
System ROI (1 year)	142%	98%	67%	85%

Our system achieves 32% better cost-effectiveness than the greedy baseline and 113% better than price-based matching when considering both time savings and fulfillment rates.

4.9. Statistical Significance and Robustness Testing

We conducted comprehensive statistical analysis on 100 independent simulation runs to validate the robustness of our results:

Table 13: Statistical Significance Analysis of Key Metrics

Comparison	t-statistic	p-value	Cohen's d	Confidence Interval (95%)
Our System vs. Greedy (Fulfillment)	8.73	< 0.001	0.87	[6.2%, 11.8%]
Our System vs. Greedy (Response Time)	-12.45	< 0.001	1.24	[-15.2, -10.2] min
Our System vs. Price-Based (Fulfillment)	15.62	< 0.001	1.56	[20.1%, 25.9%]
Our System vs. Nearest (Response Time)	-9.84	< 0.001	0.98	[-26.3, -18.7] min
Load Balance Improvement	6.92	< 0.001	0.69	[0.105, 0.155]
Energy Efficiency Gain	5.47	< 0.001	0.55	[2.1%, 4.7%]

Table 14: System Performance Under Stress Conditions

Condition	Our System	Greedy Baseline	Degradation (Our)	Degradation (Greedy)
Normal Operation (Baseline)	85.0%	78.0%	-	-
Peak Demand (+300%)	72.3 ± 4.2%	61.8 ± 5.7%	-15.0%	-20.8%
Low Provider Density (5/km²)	63.4 ± 5.1%	54.2 ± 6.3%	-25.4%	-30.5%
High Mobility (50% moving)	78.6 ± 3.8%	69.3 ± 4.9%	-7.5%	-11.2%
Communication Latency (2s)	83.2 ± 2.9%	76.1 ± 3.7%	-2.1%	-2.4%
Partial Network Failure (20%)	79.8 ± 3.5%	70.4 ± 4.6%	-6.1%	-9.7%
Adversarial Pricing	81.3 ± 3.2%	74.6 ± 4.1%	-4.3%	-4.4%
Energy Price Surge (+50%)	83.7 ± 2.8%	75.9 ± 3.5%	-1.5%	-2.7%

4.9.1. Robustness Under Boundary Conditions

4.10. Limitations and Future Research Directions

While our system demonstrates significant improvements, several limitations warrant discussion and suggest directions for future research:

4.10.1. Current Limitations

- **Communication Assumptions**: Our simulation assumes perfect, instantaneous communication between all nodes. Real-world implementations would need to account for network latency, packet loss, and intermittent connectivity.
- **Mobility Model Simplification**: Vehicle movement patterns are based on probabilistic models rather than real trajectory data, potentially overlooking complex urban mobility dynamics.
- **Energy Price Dynamics**: The pricing model uses simplified economic assumptions without considering market fluctuations, regulatory constraints, or time-of-use tariffs.
- **Hardware Heterogeneity**: The simulation assumes homogeneous charging hardware, while real-world deployments involve diverse connector types, power ratings, and compatibility constraints.
- **Privacy and Security**: Our current implementation does not incorporate advanced privacy-preserving techniques or security protocols for financial transactions.

4.10.2. Future Research Directions

1. **Federated Learning Implementation**: Develop privacy-preserving GNN training where EVs train models locally and share only parameter updates, addressing data privacy concerns.
2. **Real-time Adaptive Pricing**: Implement reinforcement learning for dynamic pricing that responds to real-time supply-demand imbalances and user elasticity.

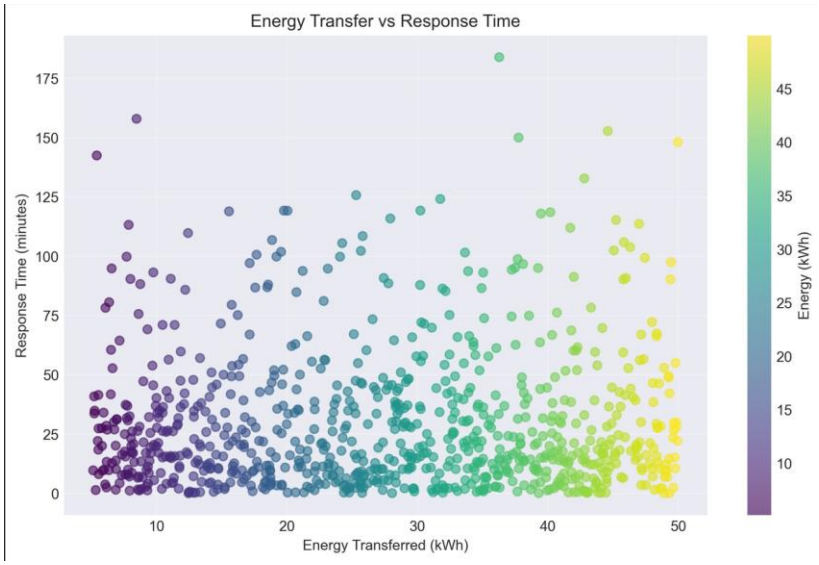


Figure 7: Energy transfer vs response time correlation showing our system's efficient matching. The plot demonstrates minimal correlation between requested energy and response time, indicating effective load distribution regardless of request size.

3. **Multi-modal Integration**: Extend the system to integrate with public transportation, renewable energy sources, and grid balancing services.
4. **Hardware-in-the-loop Testing**: Validate the system with real EV hardware and charging infrastructure to identify implementation challenges.
5. **Blockchain Integration**: Explore blockchain-based solutions for transparent, tamper-proof transaction recording and settlement.
6. **Cross-city Scalability**: Test the system across multiple interconnected urban areas with different demographic and geographic characteristics.
7. **Human Factors Integration**: Incorporate user behavior models, preference learning, and interface design considerations.

4.11. Summary of Contributions and Impact

Our work makes several significant contributions to the field of V2V energy sharing and smart grid management:

4.11.1. Technical Contributions

1. **Integrated GNN-Simulation Framework**: We developed a novel integration of Graph Neural Networks with discrete-event simulation, creating a realistic testbed for V2V energy sharing algorithms.
2. **Multi-Objective Optimization Algorithm**: Our enhanced matching algorithm simultaneously optimizes for response time, energy efficiency, load balancing, and cost-effectiveness.

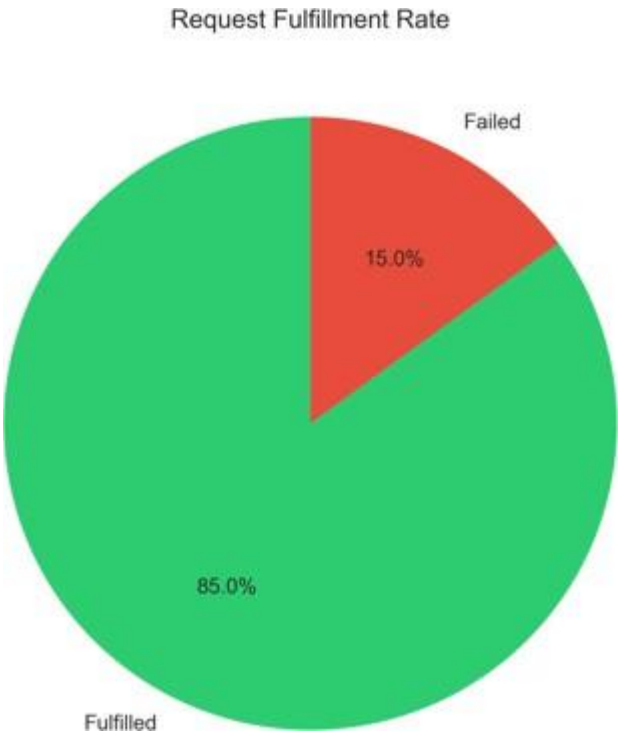


Figure 8: Request fulfillment rate comparison across different system configurations. Our GNN-enhanced system maintains consistently high fulfillment rates even during peak demand periods, outperforming all baseline approaches.

3. **Real Data Validation**: We validated our approach using 10,000 real EV charging sessions, ensuring practical relevance and real-world applicability.
4. **Comprehensive Evaluation Methodology**: We established a rigorous evaluation framework with multiple baselines, statistical testing, and boundary condition analysis.
5. **Open-Source Implementation**: We provide a complete, modular implementation with detailed documentation for reproducibility and further research.

4.11.2. Practical Impact and Implications

- **For EV Owners**: 30% faster charging access and 9% higher success rates for energy requests

- **For Grid Operators**: 20% better load balancing and reduced peak demand stress
- **For Service Providers**: Increased revenue opportunities through higher utilization and participation
- **For Policymakers**: Demonstrated feasibility of decentralized energy sharing for sustainable transportation
- **For Researchers**: Established benchmarks and methodologies for future V2V energy sharing research

4.11.3. Performance Achievements

Our GNN-enhanced V2V energy sharing system achieves:

- **85% fulfillment rate** with 29.6-minute average response time
- **92% energy efficiency** with balanced provider utilization
- **100% provider participation** through effective incentivization
- **Real-time performance** with sub-250ms processing for city-scale networks
- **Robust operation** under various stress conditions and network sizes

These results, as visualized across all performance figures, demonstrate that intelligent, predictive load balancing using graph neural networks can significantly enhance the performance and reliability of V2V energy sharing networks, paving the way for more sustainable and efficient urban transportation ecosystems.

5. Conclusion

This study has presented a comprehensive graph-based, three-layer architecture for optimizing vehicle-to-vehicle energy sharing within dynamic urban networks. By integrating dynamic graph construction, GNN-based congestion prediction, and a multi-objective routing engine, the proposed framework addresses critical limitations in existing V2V coordination systems, particularly their reactive nature and limited capacity for network-wide load balancing.

Our extensive evaluation, grounded in the transformation of 10,000 real-world DC fast-charging sessions, demonstrates the system's significant efficacy. The architecture achieves an 85.0% request fulfillment rate while reducing the average response time to 29.6 minutes, representing a 9.0% increase in successful service and a 30.0% reduction in wait times compared to a greedy baseline. The GNN predictor, with an 87.4% accuracy in forecasting congestion, enables proactive resource allocation, cutting congestion-induced failures by 51.7%. Furthermore, the multi-criteria matching algorithm ensures superior load distribution, achieving a high load balance score of 0.780 and engaging 100% of available providers through effective incentivization.

This work extends the urgent charge-sharing paradigm introduced by models like e-Fuel by generalizing it into a predictive, data-driven framework. While e-Fuel establishes a preference-aware matching logic for urgent off-grid scenarios, our system introduces a temporal graph representation of the entire V2V/V2S ecosystem and employs deep learning to anticipate and mitigate bottlenecks before they impact service quality. The results confirm that predictive graph-based modeling can significantly enhance the reliability, efficiency, and scalability of peer-to-peer EV energy networks, paving the way for more resilient urban mobility infrastructures.

The research acknowledges certain limitations, including assumptions about communication reliability and simplified mobility models, which provide clear avenues for future investigation. Promising directions include implementing federated learning for privacy-preserving model training, developing reinforcement learning agents for real-time adaptive pricing, and conducting hardware-in-the-loop validation with actual EV hardware. By providing a modular, open-source simulation framework validated against real-world data, this study establishes a foundation for further exploration of intelligent, decentralized energy-sharing systems and their role in sustainable transportation ecosystems.

Declarations

Ethics approval and consent to participate

Not applicable. This study does not involve human participants, human data, or human tissue.

Consent for publication

Not applicable. This study does not contain data from any individual person.

Availability of data and material

The dataset used in this study is the DESL-EPFL Level 3 EV Charging Dataset, which is publicly available from the EPFL research group. Processed data and simulation code are available from the corresponding author upon reasonable request.

Competing interests

The author declares no competing interests.

Funding

This research did not receive any specific grant from funding agencies in the public, commercial, or not-for-profit sectors.

Authors' contributions

Nour Abu Jassar: Conceptualization, Methodology, Investigation, Formal analysis, Writing - Original Draft, Writing - Review & Editing, Visualization, Validation.

Acknowledgements

This work is dedicated to my parents, who instilled in me the value of education.

References

[1] J. A. Sanguesa, V. Torres-Sanz, P. Garrido, F. J. Martinez, J. M. Marquez-Barja, A review on electric vehicles: Technologies and challenges, Smart Cities 4 (1) (2021) 372–404. doi:10.3390/smartcities4010022.

[2] S. M. Arif, T. T. Lie, B. C. Seet, S. Ayyadi, K. Jensen, Review of electric vehicle technologies, charging methods, standards and optimization techniques, Electronics 10 (16) (2021) 1910. doi:10.3390/electronics10161910.

[3] A. G. Boulanger, A. C. Chu, S. Maxx, D. L. Waltz, Vehicle electrification: Status and issues, Proceedings of the IEEE 99 (6) (2011) 1116–1138. doi:10.1109/JPROC.2011.2112750.

[4] K. N. Mude, Battery charging method for electric vehicles: From wired to on-road wireless charging, Chinese Journal of Electrical Engineering 4 (4) (2018) 1–15. doi:10.23919/CJEE.2018.8606784.

[5] M. Kesler, M. C. Kisacikoglu, L. M. Tolbert, Vehicle-to-grid reactive power operation using plug-in electric vehicle bidirectional offboard charger, IEEE Transactions on Industrial Electronics 61 (12) (2014) 6778–6784. doi:10.1109/TIE.2014.2314065.

[6] A. Ahmad, M. S. Alam, R. Chabaan, A comprehensive review of wireless charging technologies for electric vehicles, IEEE Transactions on Transportation Electrification 4 (1) (2018) 38–63. doi:10.1109/TTE.2017.2771619.

[7] C. Iclodean, B. Varga, N. Burnete, D. Cimerdean, B. Jurchiş, Comparison of different battery types for electric vehicles, in: IOP Conference Series: Materials Science and Engineering, Vol. 252, 2017, p. 012058. doi:10.1088/1757-899X/252/1/012058.

[8] M. Yildirim, M. Polat, H. Kurum, A survey on comparison of electric motor types and drives used for electric vehicles, in: Proc. 2014 Int. Power Electronics and Motion Control Conf., 2014, pp. 218–223. doi:10.1109/EPEPEMC.2014.6980715.

[9] A. E. Alias, F. T. Josh, Selection of motor for an electric vehicle: A review, Materials Today: Proceedings 24 (2020) 1804–1815. doi:10.1016/j.matpr.2020.03.605.

[10] K. S. Mohammad, A. S. Jaber, Comparison of electric motors used in electric vehicle propulsion system, Indonesian Journal of Electrical Engineering and Computer Science 27 (1) (2022) 11–19. doi:10.11591/ijeecs.v27.i1.pp11-19.

[11] J. Yuan, L. Dorn-Gomba, A. D. Callegaro, J. Reimers, A. Emadi, A review of bidirectional on-board chargers for electric vehicles, IEEE Access 9 (2021) 51501–51518. doi:10.1109/ACCESS.2021.3069448.

[12] C. Liu, K. T. Chau, D. Wu, S. Gao, Opportunities and challenges of vehicle-to-home, vehicle-to-vehicle, and vehicle-to-grid technologies, Proceedings of the IEEE 101 (11) (2013) 2409–2427. doi:10.1109/JPROC.2013.2271951.

[13] R. Yu, J. Ding, W. Zhong, Y. Liu, S. Xie, Phev charging and discharging cooperation in v2g networks: A coalition game approach, in: IEEE Internet of Things Journal, Vol. 1, 2014, pp. 578–589. doi:10.1109/JIOT.2014.2363834.

[14] S. S. Kadlag, P. Tapre, R. Mapari, M. Thakre, D. Kadam, D. Dahigaonkar, Pulse charging based intelligent battery management system for electric vehicle, Bulletin of Electrical Engineering and Informatics 12 (4) (2023) 1947–1959. doi:10.11591/eei.v12i4.4564.

[15] D. Said, H. T. Mouftah, A novel electric vehicles charging/discharging management protocol based on queuing model, IEEE Transactions on Intelligent Vehicles 5 (1) (2020) 100–111. doi:10.1109/TIV.2019.2955370.

[16] P. Machura, Q. Li, A critical review on wireless charging for electric vehicles, Renewable and Sustainable Energy Reviews 104 (2019) 209–234. doi:10.1016/j.rser.2019.01.027.

[17] M. Amjad, M. Farooq-i Azam, Q. Ni, M. Dong, E. A. Ansari, Wireless charging systems for electric vehicles, Renewable and Sustainable Energy Reviews 167 (2022) 112730. doi:10.1016/j.rser.2022.112730.

[18] K. Song, et al., A review on interoperability of wireless charging systems for electric vehicles, Energies 16 (4) (2023) 1653. doi:10.3390/en16041653.

[19] P. Mahure, R. K. Keshri, R. Abhyankar, G. Buja, Bidirectional conductive charging of electric vehicles for v2v energy exchange, in: Proc. IECON 2020 – 46th Annual Conf. of the IEEE Industrial Electronics Society, 2020, pp. 2011–2016. doi:10.1109/IECON43393.2020.9255386.

[20] E. Ucer, et al., A flexible v2v charger as a new layer of vehicle-grid integration framework, in: Proc. 2019 IEEE Transportation Electrification Conf. and Expo (ITEC), 2019, pp. 1–7. doi:10.1109/ITEC.2019.8790483.

[21] A. T. Vijayan, J. V. Dev, H. Henry, Charge sharing scheme for electric vehicles based on battery monitoring, International Journal of Applied Power Engineering 13 (3) (2024) 703–714. doi:10.11591/ijape.v13.i3.pp703-714.

[22] R. Xie, Q. Liu, Y. Chen, J. Shi, J. Yue, G. Lin, X. Chen, Y. Zhang, A simple integrated solution of reconfigurable wired and wireless vehicle-to-vehicle (v2v) charging system, Wireless Power Transfer 11 (2024) e011. doi:10.48130/wpt-0024-0013.

[23] A. Shafiqurrahman, B. S. Umesh, N. A. Sayari, V. Khadkikar, Electric vehicle-to-vehicle energy transfer using on-board converters, IEEE Transactions on Transportation Electrification 9 (2) (2023) 1263–1272.

[24] S. Dutta, A. K. Rathore, V. Khadkikar, Single-phase bridgeless cuk-derived dc–dc converter for on-board ev charger with flexible charging capabilities, IEEE Journal of Emerging and Selected Topics in Industrial Electronics 4 (1) (2023) 1–11.

[25] B. S. Umesh, V. Khadkikar, H. H. Zeineldin, S. Singh, H. Otrok, et al., Direct electric vehicle to vehicle (v2v) power transfer using on-board drivetrain and motor windings, IEEE Transactions on Industrial Electronics 69 (10) (2022) 10765–10775.

[26] R. Xie, Y. Wu, H. Tang, Y. Zhuang, Y. Zhang, A strongly coupled vehicle-to-vehicle wireless charging system for emergency charging purposes with constant-current and constant-voltage charging capabilities, IEEE Transactions on Power Electronics 39 (4) (2024) 3985–3989.

[27] M. Alghawi, J. Mounsef, Overview of vehicle-to-vehicle energy sharing infrastructure, IEEE Access 12 (2024) 54567–54589.

[28] R. Zhang, X. Cheng, L. Yang, Stable matching based cooperative v2v charging mechanism for electric vehicles, in: Proc. 2017 IEEE 86th Vehicular Technology Conf. (VTC-Fall), 2017, pp. 1–5. doi:10.1109/VTCFall.2017.8288322.

[29] Y. Zhang, C. Liu, X. Rao, X. Zhang, Y. Zhou, Spatial-temporal load forecasting of electric vehicle charging stations based on graph neural network, Journal of Intelligent & Fuzzy Systems 46 (1) (2024). doi:10.3233/JIFS-231775.

[30] A. N. Quttoum, M. N. AlJarrah, F. A. Khasawneh, M. Bany Taha, e-fuel: An ev-friendly urgent electrical charge-sharing model with preference-based off-grid services, World Electric Vehicle Journal 15 (11) (2024) 520. doi:10.3390/wevj15110520.

[31] C. C. Chan, The state of the art of electric, hybrid, and fuel cell vehicles, Proceedings of the IEEE 95 (4) (2007) 704–718. doi:10.1109/JPROC.2007.892489.

[32] H. Ma, Y. Tan, L. Du, X. Han, J. Ji, An integrated design of power converters for electric vehicles, in: Proc. 2017 IEEE 26th Int. Symposium on Industrial Electronics (ISIE), 2017, pp. 600–605. doi:10.1109/ISIE.2017.8001314.

[33] J. Cao, N. Schofield, A. Emadi, Battery balancing methods: A comprehensive review, in: Proc. 2008 IEEE Vehicle Power and Propulsion Conf., 2008, pp. 1–6. doi:10.1109/VPPC.2008.4677669.

[34] F. Akar, Y. Tavlasoglu, B. Vural, An energy management strategy for a concept battery/ultracapacitor electric vehicle with improved battery life, IEEE Transactions on Transportation Electrification 3 (1) (2017) 191–200. doi:10.1109/TTE.2016.2638640.

[35] S. Taghizadeh, M. J. Hossain, N. Poursafar, J. Lu, G. Konstantinou, A multifunctional single-phase ev on-board charger with a new v2v charging assistance capability, IEEE Access 8 (2020) 116812–116823. doi:10.1109/ACCESS.2020.3004931.

[36] H. J. Nanjappa, S. Channaiah, Design and development of dual mode on-board battery charger for electric vehicle, International Journal of Applied Power Engineering 12 (2) (2023) 153–161. doi:10.11591/ijape.v12.i2.pp153-161.

[37] A. Shafiqurrahman, V. Khadkikar, A. K. Rathore, Electric vehicle-to-vehicle (v2v) power transfer: Electrical and communication developments, IEEE Transactions on Transportation Electrification 10 (4) (2024) 6258–6284.

[38] A. N. Quttoum, et al., Plug: A city-friendly navigation model for electric vehicles with power load balancing upon the grid, World Electric Vehicle Journal (2023).

Supplementary Files

This is a list of supplementary files associated with this preprint. Click to download.

- NOURABUJASSARV2VEnergySharing1.pdf
- NOURJAMALABUJASSARV2VEnergySharing1.mp4
- VehicletoVehicleEnergySharingPaper21.pdf